Effective Lennard-Jones Parameters for CO_2-CO_2 Dispersion Interactions in Water and near Amorphous Silica-water Interfaces

P. Thiyam[1], **O. I. Malyi**[2], **C. Persson**[1, 2, 3], **S. Y. Buhmann**[4, 5], **D. F. Parsons**[6], **and M. Boström**[2]

[1]Department of Materials Science and Engineering
Royal Institute of Technology, SE-100 44 Stockholm, Sweden
[2]Centre for Materials Science and Nanotechnology
University of Oslo, P. O. Box 1048, Blindern, NO-0316 Oslo, Norway
[3]Department of Physics, University of Oslo, P. O. Box 1048, Blindern, NO-0316 Oslo, Norway
[4]Physikalisches Institut, Albert-Ludwigs-Universität Freiburg
Hermann-Herder-Str. 3, 79104 Freiburg, Germany
[5]Freiburg Institute for Advanced Studies, Albert-Ludwigs-Universität Freiburg
Albertstraβe 19, 79104 Freiburg, Germany
[6]School of Engineering and IT, Murdoch University, 90 South St, Murdoch, WA 6150, Australia

Abstract— Different models for effective polarizability in water and the corresponding dispersion forces between dissolved molecules are explored in bulk water and near interfaces. We demonstrate that the attractive part of the Lennard-Jones parameters, i.e., the van der Waals parameter C_6 ($U_{vdW} \approx -C_6/\rho^6$), is strongly modified when two carbon dioxide (CO_2) molecules are near an amorphous silica-water and near a vapor-water interface. Standard simulation parameters for near-surface modeling are based on intermolecular forces in bulk media.

1. INTRODUCTION

Tight rocks may provide most of the world's future fossil energy. New production methods that allow hydrocarbons to be produced directly from tight source rocks such as shale gas and shale oil systems have changed the world's energy outlook [1]. We are now at a stage where the technology for recovery has advanced beyond our scientific understanding of the underlying processes. This creates new opportunities for technological and scientific innovations. Much fundamental research focus on molecular physisorption/chemisorption and meso-scale transport processes in nanostructured shales. By understanding the underlying physical processes, the ultimate aim of such research is to realize a controlled conversion process of carbon dioxide(CO_2) to methane (CH_4) in model porous media and more generally in hydrofractured shale.

The fluctuation of the electromagnetic field in the vicinity of a molecule near a surface, or between surfaces, is different from that in free space giving rise to different interactions [2]. Using the formalism of Sambale et al. [4], we explore how the presence of interfaces influence intermolecular forces between a pair of CO_2 molecules. Traditional Lennard-Jones parameters are derived from intermolecular forces in bulk media. However, we show that the attractive part of the Lennard-Jones potential (i.e., the van der Waals attraction) changes near interfaces. It depends on the properties of the materials involved, the model of polarizability of the molecule used and the relative orientation of the molecules near the interface. The dispersion forces between dissolved CO_2 molecules are explored in bulk water and near amorphous silica-water and air-water interfaces using different models for effective polarizability, viz. the hardsphere model and Onsager's model [3].

In the next section, we first briefly describe the interaction of a single molecule in a medium with a surface. In Section 3, we discuss the theory of interaction of two molecules embedded in a medium near a surface. In Section 4, we briefly describe the two models of effective polarizability of the molecule in water. In Section 5, we explain the modeling of the dielectric functions of the background medium (water) and the surface of amorphous silica. We provide the van der Waals C_6 parameters for CO_2-CO_2 interaction in bulk water using different models of polarizability in Section 6. In Section 7, we present our main analysis and results. We end with a few conclusions in Section 8.

2. VAN DER WAALS ENERGY OF A SINGLE MOLECULE NEAR A WATER-SILICA INTERFACE

We explore the formalism due to Buhmann and co-workers for local field corrections when small carbon dioxide (CO_2) molecules are in a media [2–6]. The distance-dependent part of the retarded

van der Waals potential [2] of a polarizable molecule in water near an interface [4] is,

$$U(z) = k_B T {\sum_{n=0}^{\infty}}' \alpha_w(i\xi_n) \int_0^\infty \frac{dqq(f^p + f^s)}{\gamma_0}, \tag{1}$$

$$f^s = \xi_n^2 r_s \exp[-2\gamma_0 z]/c^2, \tag{2}$$

$$f^p = -\left(\frac{\xi_n^2}{c^2} + \frac{2q^2}{\epsilon_w}\right) r_p \exp[-2\gamma_0 z], \tag{3}$$

with the reflection coefficients of the interface,

$$\begin{aligned} r_s &= (\gamma_0 - \gamma_1)/(\gamma_0 + \gamma_1), \\ r_p &= (\epsilon\gamma_0 - \epsilon_w\gamma_1)/(\epsilon\gamma_0 + \epsilon_w\gamma_1), \quad \gamma_0 = \sqrt{q^2 + \epsilon_w\xi_n^2/c^2}, \\ \gamma_1 &= \sqrt{q^2 + \epsilon\xi_n^2/c^2}. \end{aligned} \tag{4}$$

Here ϵ_w and ϵ are the dielectric functions of water and the substrate respectively, and c is the velocity of light in vacuum. We define k_B as the Boltzmann constant and T is the temperature, and the prime indicates that the $n = 0$ term should be divided by 2. Furthermore $\alpha_w(i\xi_n)$ is the water-embedded molecular polarizability at the Matsubara frequencies $\xi_n = 2\pi k_B T n/\hbar$ [2, 7–9]. Here we consider systems at room temperature ($T = 300\,\mathrm{K}$).

3. EFFECT OF BACKGROUND MEDIA AND INTERFACES ON LONG-RANGE VAN DER WAALS FORCES

The presence of surfaces influences the van der Waals interaction between two molecules near an interface [5, 6]. At large CO_2-CO_2 separations the retarded van der Waals interaction between two molecules near a solid-water interface is

$$U_{vdW}(\bar{\rho}_a, \bar{\rho}_b) \approx -k_B T {\sum_{n=0}^{\infty}}' \alpha_w(i\xi_n)^2 \times \left\{ \left[\sum_{j=x,y,z} T_{jj}(\bar{\rho}_a, \bar{\rho}_b | i\xi_n)^2 \right] - 2T_{xz}(\bar{\rho}_a, \bar{\rho}_b | i\xi_n)^2 \right\}, \tag{5}$$

where $\bar{\rho}_{a,b}$ are the positions of the two molecules with respect to a fixed point at the interface, and the other factors are as described in the previous section. We study van der Waals interaction near amorphous silica-water interface and air-water interface. The susceptibility tensor element (T_{jj}) is a sum of contributions from bulk water susceptibility (T_{jj}^0), plus p (T_{jj}^{1p}) and s (T_{jj}^{1s}) interface corrections.

The susceptibility tensor elements for two polarizable particles near solid-air interfaces are well studied in the literature [10, 11]. Here we present the theory with arbitrary orientations for two CO_2 molecules in water near an amorphous silica-water interface. We consider only distances much larger than two radii where finite size effects can be neglected [12]. We consider the case when x is the distance between the two molecules parallel to the surface and z_a and z_b are the distances of atoms a and b from the surface.

We consider the general case where the two interacting CO_2 molecules are not situated in free space, but embedded in a water medium near a solid-water interface. The presence of the water medium modifies the van der Waals interaction in different ways: Firstly, the non-trivial refractive index of water $\tilde{n} = \tilde{n}(\mathrm{i}\xi_n) = \sqrt{\epsilon_w(\mathrm{i}\xi_n)}$ leads to a modified light propagation. As a result, the free-space susceptibility is replaced with its counterpart in a bulk water medium

$$\begin{aligned} T_{xx}^0 &= (A - Bx^2/d^2)e^{-\tilde{n}\xi_n d/c}/(\epsilon_w d^3), \\ T_{yy}^0 &= Ae^{-\tilde{n}\xi_n d/c}/(\epsilon_w d^3), \\ T_{zz}^0 &= [A - Bz_m^2/(d^2)]e^{-\tilde{n}\xi_n d/c}/(\epsilon_w d^3) \end{aligned} \tag{6}$$

with

$$\begin{aligned} A &= 1 + (d\tilde{n}\xi_n/c) + (d\tilde{n}\xi_n/c)^2, \\ B &= 3 + (3d\tilde{n}\xi_n/c) + (d\tilde{n}\xi_n/c)^2, \\ d &= \sqrt{x^2 + z_-^2}. \end{aligned} \tag{7}$$

Here, we define $z_+ = z_a + z_b$ and $z_- = z_a - z_b$ with the first being the distance between molecule a and the image of molecule b inside the surface and the second being distance between the two molecules.

The corresponding surface-induced corrections to the susceptibility matrix [10, 11] have contributions from p and s polarizations,

$$\begin{aligned}
T_{xx}^{1s} &= \int_0^\infty dq(\xi_n^2/c^2)(q/\gamma_0)e^{-\gamma_0 z_+} r_s[J_0(qx) + J_2(qx)]/2, \\
T_{yy}^{1s} &= \int_0^\infty dq(\xi_n^2/c^2)(q/\gamma_0)e^{-\gamma_0 z_+} r_s[J_0(qx) - J_2(qx)]/2, \\
T_{zz}^{1s} &= 0,
\end{aligned} \tag{8}$$

$$\begin{aligned}
T_{xx}^{1p} &= -\int_0^\infty dqq\gamma_0 e^{-\gamma_0 z_+} r_p[J_0(qx) - J_2(qx)]/2, \\
T_{yy}^{1p} &= -\int_0^\infty dqq\gamma_0 e^{-\gamma_0 z_+} r_p[J_0(qx) + J_2(qx)]/2, \\
T_{zz}^{1p} &= -\int_0^\infty dq(q^3/\gamma_0)e^{-\gamma_0 z_+} r_p J_0(qx), \\
T_{xz(zx)}^{1p} &= \mp\int_0^\infty dqq^2 e^{-\gamma_0 z_+} r_p J_1(qx),
\end{aligned} \tag{9}$$

with the reflection coefficients of the interface,

$$\begin{aligned}
r_s &= (\gamma_0 - \gamma_1)/(\gamma_0 + \gamma_1), \\
r_p &= (\epsilon\gamma_0 - \epsilon_w\gamma_1)/(\epsilon\gamma_0 + \epsilon_w\gamma_1), \quad \gamma_0 = \sqrt{q^2 + \epsilon_w\xi_n^2/c^2}, \\
\gamma_1 &= \sqrt{q^2 + \epsilon\xi_n^2/c^2}.
\end{aligned} \tag{10}$$

4. TWO MODELS FOR EFFECTIVE POLARIZABILITY OF MOLECULES IN WATER

The macroscopic electromagnetic field in a medium is different from the local field acting on a molecule. This can be accounted for via Onsager's real-cavity model [13]. Assuming that the molecule surrounded by a small spherical vacuum bubble, one can show [3] that local-field corrections lead to a replacement of the CO_2 free-space polarizability with their water-embedded counterparts

$$\alpha_w = \alpha\left(\frac{3\epsilon_w}{2\epsilon_w + 1}\right)^2 \tag{11}$$

where

$$\alpha(i\omega_n) = \alpha(0)\sum_j \frac{f_j}{1 + (\omega_n/\omega_j)^2}, \tag{12}$$

is replaced with the dynamic free-space polarizability obtained from ab initio calculations [14, 15]. The other model of polarizability of the molecule that we consider is the hardsphere model that treats the molecule as a homogeneous dielectric sphere of radius a. Its effective permittivity ϵ can be deduced from the free-space polarizability (12) via [16]

$$\alpha = a^3\,\frac{\epsilon - 1}{\epsilon + 2}\,. \tag{13}$$

The excess polarizability of the homogeneous-sphere molecule in water is then [17]

$$\alpha_w = \epsilon_w a^3\,\frac{\epsilon - \epsilon_w}{\epsilon + 2\epsilon_w}\,. \tag{14}$$

5. THE DIELECTRIC FUNCTIONS OF WATER AND AMORPHOUS SILICA

The dielectric function on the imaginary axis was obtained from the imaginary part of the function, and using the following version of the Kramers-Kronig dispersion relation

$$\varepsilon(i\xi) = 1 + \frac{2}{\pi}\int_0^\infty d\omega \frac{\omega\varepsilon_2(\omega)}{\omega^2+\xi^2}. \tag{15}$$

This relation is the result of the analytical properties of the dielectric function [9]. In the integration we made a cubic spline interpolation of $\ln(\varepsilon_2(\omega))$ as a function of $\ln(\omega)$. The dielectric function of water [9] at room temperature ($T = 300K$) was based on the extensive experimental data found in Ref. [18].

The dielectric properties of amorphous silica were calculated using scissors-operator approximation (Δ=3.6) for Perdew-Burke-Ernzerhof (PBE) density functional theory (DFT) calculations. The dielectric function on the imaginary frequency axis was determined from the Kramers-Kronig dispersion relation. The low-energy spectra are verified by calculating the static dielectric constants from the Born effective charges. The static dielectric constant was found to be 4.08 ± 0.11. All calculations were carried out using the Vienna ab initio simulation package (VASP) with the Perdew-Burke-Ernzerhof (PBE) [19] functional. Projector augmented wave (PAW) pseudopotentials [20, 21] were used to model the effect of core electrons. The non-local parts of the pseudopotentials were treated in real and reciprocal space Born-Oppenheimer molecular dynamics (BOMD) and all other density functional theory (DFT) calculations, respectively. The cutoff energy for plane wave basis set was set to 400 and 300 eV for all static DFT and BOMD calculations, respectively. It should be noted that for BOMD, to make sure that the cutoff energy does not affect final energetics and electronic/optical properties, one of the amorphous samples was prepared using 400 eV as the cutoff energy (the calculations were performed for third annealing/quenching temperature protocol only, see below). To generate the amorphous structure, BOMD simulations with three different annealing/quenching temperature protocols were used. For all temperature protocols, atomic velocities were initialized at 5000 K using the Maxwell-Boltzmann distribution. Then, the system was melted and annealed for the period of 10 ps. The resulted system was quenched to 2500 K during the periods of 2.5 ps, 5 ps, and 10 ps for first, second, and third annealing/quenching temperature protocols, respectively. Then the systems were annealed for a period of 10 ps and finally were quenched to 1 K for a period of 30 ps. In all simulations, time step was set to 1 fs. It should be noted that the structure annealing was carried out using canonical ensemble BOMD (number of atoms, volume, and temperature was conserved). For all BOMD simulations, the system temperature was controlled using the Nosé thermostat [22–24]. The obtained structures were further fully optimized using quasi-Newton algorithm. Among four generated systems, the highest energy structure was not used for further calculations due to stabilisation of high energy local defects. The computed average band gaps for the amorphous structure was found to be 5.33 ± 0.01 eV.

6. CO_2 VAN DER WAALS PARAMETERS IN BULK WATER

The effective van der Waals parameter C_6 ($U_{vdW} \approx -C_6/\rho^6$) for the interaction of a pair of CO_2 molecules in bulk water is found to be -1.10×10^{-58} erg.cm^6 for the Onsager's model of polarizability and -0.78×10^{-58} erg.cm^6 for the hardsphere model of polarizability. We will show in the next section that this C_6 parameter is strongly modified in the presence of a surface. The C_3 coefficients for the interaction of a single CO_2 molecule with amorphous silica and air surfaces are given in Table 1.

Table 1: The C_3 values (the non-retarded van der Waals energy times z^3 in units of 10^{-37}erg.cm^3) for CO_2-surface interaction for the hard sphere and Onsager's models near different interfaces. a-SiO_2 here refers to amorphous silica.

Interface	C_3 (Onsager)	C_3 (Hardsphere)
a-SiO_2-water	-4.43	-3.77
air-water	12.72	10.58

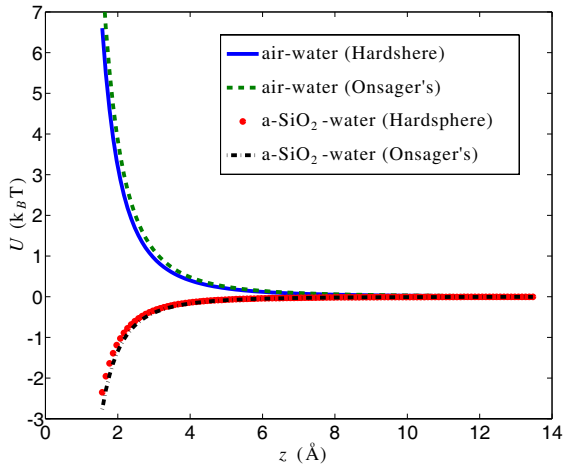

Figure 1: The non-retarded van der Waals energy in units of k_BT of a CO_2 molecule near amorphous silica-water interface and near air-water interface for the hardsphere and Onsager's models of polarizability (at $T = 300\,\mathrm{K}$). Amorphous silica is written in short as a-SiO_2 in this figure and the following ones.

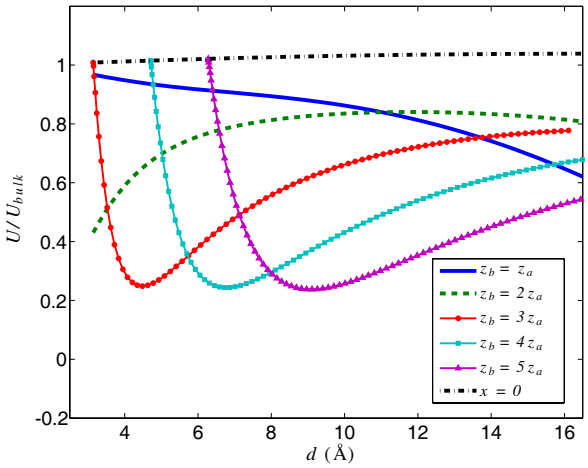

Figure 2: The ratio between the retarded van der Waals potential near an amorphous silica-water interface and the non-retarded van der Waals potential in bulk water of two CO_2 molecules with Onsager's model of polarizability (at $T = 300\,\mathrm{K}$). $z_a = 1.57$Å.

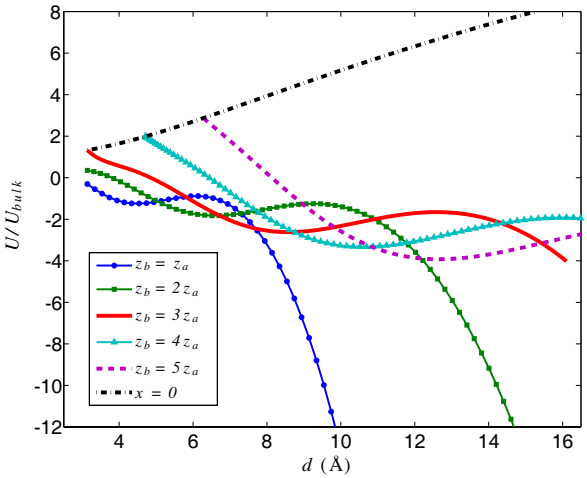

Figure 3: The ratio between the retarded van der Waals potential near an amorphous silica-water interface and the non-retarded van der Waals potential in bulk water of two CO_2 molecules with hardsphere model of polarizability (at $T = 300\,\mathrm{K}$). $z_a = 1.57$ Å.

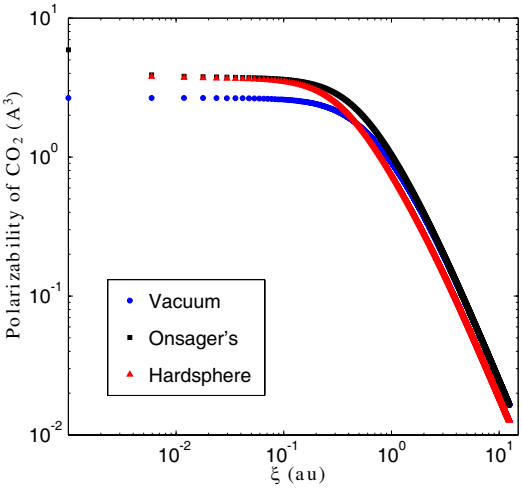

Figure 4: The polarizability of CO_2 in vacuum and the Onsager's and hardsphere models of polarizability of a CO_2 molecule in water in units of $\mathrm{Å}^3$. The polarizabilities are shown only at the room temperature Matsubara frequencies. The vacuum and Onsager's polarizability values for $\xi = 0$ are shown on the y-axis. The corresponding value for the hardsphere model at $\xi = 0$ is -129.83 $\mathrm{Å}^3$.

7. SURFACE EFFECTS ON EFFECTIVE VAN DER WAALS PARAMETERS

In Fig. 1, we present the non-retarded van der Waals energy of a CO_2 molecule in water near amorphous silica and air surfaces as a function of molecule-surface separation distance. The two models of effective polarizability, namely the hardsphere and Onsager's models of polarizability behave very much the same for single molecule-surface interaction. In Fig. 2, we show the ratio of the retarded van der Waals potential U_{vdW} of two CO_2 molecules in water interacting near an amorphous silica surface at room temperature to the non-retarded van der Waals potential U_{bulk} of two CO_2 molecules interacting in bulk water in the absence of any surface. The first molecule is at the interface, i.e., z_a is fixed at a distance of one radius from the surface while the other molecule is placed at different positions in the medium ($z_b = z_a, 2z_a, 3z_a, 4z_a, 5z_a$). Varying x then

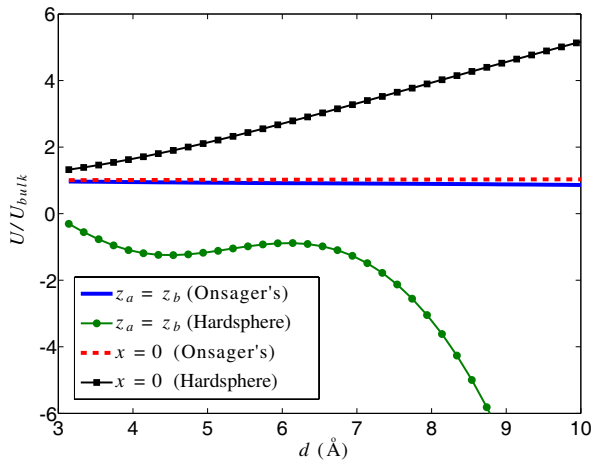

Figure 5: Comparisons of the ratio of interactions near an amorphous silica-water interface and in bulk water of two CO_2 molecules with the two different models of polarizability (at $T = 300\,\mathrm{K}$). The orientations considered here are for $z_a = z_b = 1.57$ Å and for $x = 0$.

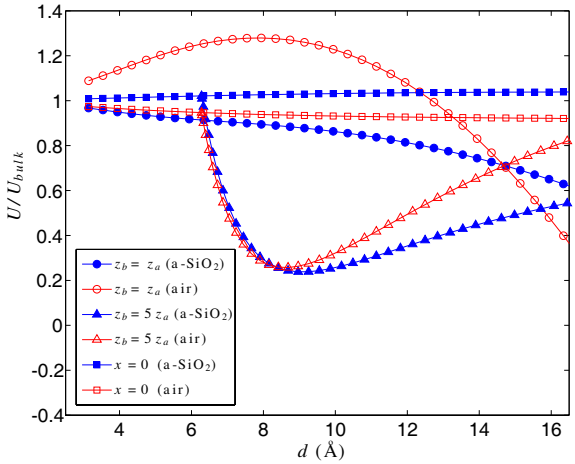

Figure 6: Comparisons of the ratio of interactions near an amorphous silica-water interface and near air-water interface of two CO_2 molecules with Onsager's model of polarizability (at $T = 300\,\mathrm{K}$) for three different types of orientations.

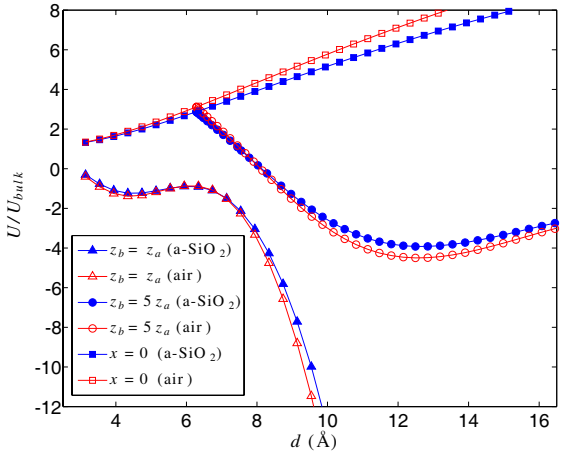

Figure 7: Comparisons of the ratio of interactions near an amorphous silica-water interface and near air-water interface of two CO_2 molecules with hard sphere model of polarizability (at $T = 300\,\mathrm{K}$) for three different types of orientations.

gives varying separation distances d between the two molecules. The model of polarizability of the molecules used is Onsager's model. In Fig. 3, we show similar plots but for the hardsphere model of polarizability. For both the hardsphere and Onsager's models of polarizability, we observe surface effects due to the presence of the amorphous silica surface. Depending on the orientation, we see that the ratio is larger or smaller than one. For the Onsager model of polarizability, the effect of the surface is minimum at the orientation $x = 0$, i.e., when the molecules are aligned perpendicular to the surface as shown by the very slight deviation from ratio 1 in Fig. 2 while in the hardsphere model, nothing conclusive can be said about which orientation is least or most affected by the surface. Another interesting observation is that the CO_2 molecules even repulse each other for the hardsphere model of polarizability (see Fig. 3) In this model, the polarizability of the molecule in the medium is the excess polarizability between the polarizability of the molecule and that of the medium. Since water is polar, its polarizability at zero frequency is large. The excess polarizability then becomes negative and the molecular sphere is essentially like a bubble. This is relevant at large distances where the zero-frequency contribution becomes dominant. At such retarded distances, the hardsphere molecule behaves like a void or bubble, and the repulsive force is analogous to negative gravity experienced by an air bubble rising in water. The hardsphere polarizability does not converge or converges very slowly to the free-space value for high frequencies.

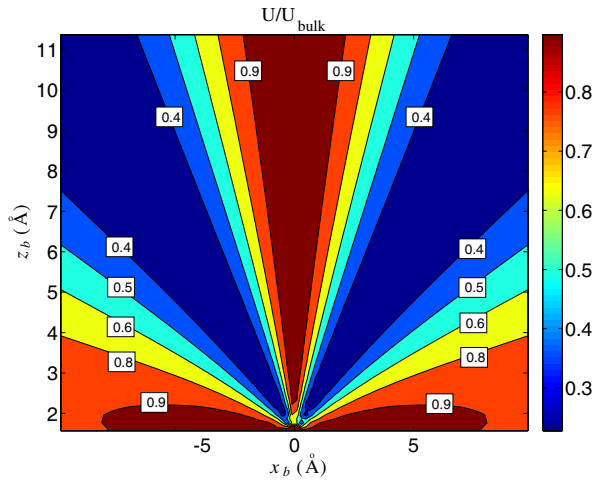

Figure 8: Contour plot showing the U/U_{bulk} ratio profile for Onsager's model of polarizability when z_a is fixed at one molecule radius from amorphous silica-water interface, i.e., $z_a = 1.57$ Å while the second molecule continuously changes position.

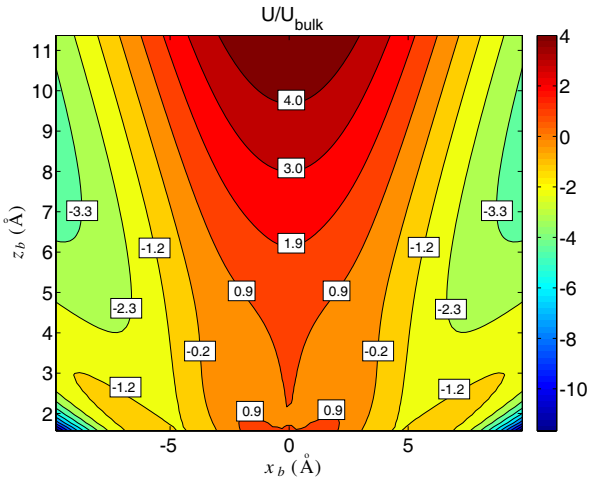

Figure 9: Contour plot showing the U/U_{bulk} ratio profile for the hardsphere model of polarizability when z_a is fixed at one molecule radius from amorphous silicaa-water interface, i.e., $z_a = 1.57$ Å while the second molecule continuously changes position.

(see Fig. 4). In Fig. 4, we present the polarizability curve of CO_2 molecule in vacuum and the curves for the two models of polarizabilty of a CO_2 molecule in water for Matsubara frequencies at room temperature. In the Onsager model, the molecule has a strictly positive polarizability inside a vacuum bubble. The effect of the bubble is a moderate enhancement of the polarizability of upto 1.5 for infinite host-medium ϵ. For large frequencies and hence smaller ϵ, the factor converges to one and the polarizability then agrees with that in vacuum. Fig. 5 more clearly demonstrates the difference in behaviour of the ratio curves for the two models of polarizability shown here for two different types of orientation, namely, the $z_a - z_b = 0$ orientation in which the molecules are aligned parallel to the surface and $x = 0$ orientation in which the molecules are aligned perpendicular to the surface. To study the effects of different types of surfaces, we compare the interactions when the two CO_2 molecules are near an amorphous silica-water interface and near air-water interface for the orientations $x = 0$, $z_b = z_a$ and $z_b = 5z_a$ using Onsager's model and the hardpshere model in Figs. 6 and 7 respectively. Contour plots 8 and 9 show the ratio profile when the first molecule is fixed at the interface while the position of the second molecule is varied.

8. CONCLUSIONS

Lennard-Jones parameters for CO_2-CO_2 interactions used in simulations on near-surface modeling are based on intermolecular forces in bulk media. We have demonstrated that such work based on CO_2-CO_2 van der Waals interaction in bulk water may be misleading for simulations near interfaces. The van der Waals interaction may even turn repulsive near amorphous silica-water interfaces for the hardsphere model of polarizability in sharp contrast to the interaction in bulk media.

ACKNOWLEDGMENT

PT acknowledges support from the European Commission. MB, OM, and CP acknowledge support from the Research Council of Norway (Project: 221469). CP acknowledges support from the Swedish Research Council (Contract No. C0485101). We acknowledge access to high-performance computing resources via SNIC/SNAC and NOTUR. SYB gratefully acknowledges support by the German Research Council (grant BU 1803/3-1).

REFERENCES

1. Sapag, K., A. Vallone, A. García Blanco, and C. Solar, "Adsorption of methane in porous materials as the basis for the storage of natural gas," *Natural Gas*, Primoz Potocnik, Ed., 2010.
2. Mahanty, J. and B. W. Ninham, *Dispersion Forces*, Academic, London, 1976.
3. Sambale, A., S. Y. Buhmann, D.-G. Welsch, and M. S. Tomas, *Phys. Rev. A*, Vol. 75, 042109, 2007.

4. Sambale, A., D.-G. Welsch, Ho Trung Dung, and S. Y. Buhmann, *Phys. Rev. A*, Vol. 79, 022903, 2009.
5. Buhmann, S. Y., *Dispersion Forces I: Macroscopic Quantum Electrodynamics and Ground-State Casimir, Casimir–Polder and van der Waals Forces*, Springer, Heidelberg, 2012.
6. Buhmann, S. Y., *Dispersion Forces II: Many-Body Effects, Excited Atoms, Finite Temperature and Quantum Friction*, Springer, Heidelberg, 2012.
7. Lifshitz, E. M., *Zh. Eksp. Teor. Fiz.*, Vol. 29, 94, 1955.
8. Lifshitz, E. M., *Sov. Phys. JETP*, Vol. 2, 73, 1956.
9. Sernelius, B. E., *Surface Modes in Physics*, Wiley, Berlin, 2001.
10. Safari, H., S. Y. Buhmann, D.-G. Welsch, and H. T. Dung, *Phys. Rev. A*, Vol. 74, 042101, 2006.
11. Buhmann, S. Y., H. Safari, H. T. Dung, and D.-G. Welsch, *Optics and Spectroscopy*, Vol. 103, 374, 2007.
12. Thiyam, P., C. Persson, B. E. Sernelius, D. F. Parsons, A. Malthe-Sørenssen, and M. Boström, *Phys. Rev. E*, in press, 2014.
13. Onsager, L., *J. Am. Chem. Soc.*, Vol. 58, 1486, 1936.
14. Parsons, D. F. and B. W. Ninham, *J. Phys. Chem. A*, Vol. 113, 1141, 2009.
15. Parsons, D. F. and B. W. Ninham, *Langmuir*, Vol. 26, 1816, 2010.
16. Jackson, J. D., *Classical Electrodynamics*, Wiley, New York, 1998.
17. Sambale, A., S. Y. Buhmann, and S. Scheel, *Phys. Rev. A*, Vol. 81, 012509, 2010.
18. Querry, M. R., D. M. Wieliczka, and D. J. Segelstein, *Handbook of Optical Constants of Solids II*, 1059, Academic Press, 1991.
19. Perdew, J. P., K. Burke, and M. Ernzerhof, *Phys. Rev. Lett.*, Vol. 77, 3865, 1996.
20. Kresse, G. and D. Joubert, *Phys. Rev. B*, Vol. 59, 1758, 1999.
21. Blöchl, P. E., *Phys. Rev. B*, Vol. 50, 17953, 1994.
22. Nosé, S., *Mol. Phys.*, Vol. 52, 255, 1984.
23. Hoover, W. G., *Physical Review A*, Vol. 31, 1695, 1985.
24. Nosé, S., *J. Chem. Phys.*, Vol. 81, 511, 1984.